

## OPTIMIZATION OF A DUAL ONE-TURN COILS KICKER MAGNET SYSTEM

K.L. Tsai\*, C.S. Fann, H.M. Shih, S.Y. Hsu, Y.S. Wong, Y.D. Li, K.B. Liu, K.K. Lin, C.T. Chen  
NSRRC, Hsinchu, Taiwan

### Abstract

Optimization of a dual one-turn coils configuration for fast kicker magnet system is presented in this report. Emphasis has been made on the: 1) optimization of various possible coils arrangement restricted by the existing available hardware; and 2) synchronization between pulsed currents delivering on the respective upper and lower coils. In the consideration of coils arrangement, good field region is utilized as the guiding parameter while adjusting fixture gap between the coils. As for coil currents timing optimization, fast rise-time and pulse shape preservation are chosen as monitoring parameters for practical implementation purpose. Both numerical analysis and experimental results are presented and discussed.

### INTRODUCTION

The fast magnetic kicker systems have been widely used in synchrotron light sources for decades. Recently, research groups have developed a fast-rise kicker magnet system operating in saturation region [1, 2] and a bridged-T network lumped kicker for a compact synchrotron application [3].

In the case of fast-rising field is required within a limited available space, e.g., dimensions of kicker magnet length and the ceramic chamber are constrained by the design of beam extraction scheme and hardware integration, a dual one-turn coils configuration of the kicker magnet can usually cope with need.

This suggested configuration, in comparison with a typical two-turn coil configuration, is able to reduce the rise-time of the pulse field effectively [4].

The optimization of the dual one-turn coils for a kicker magnet has been further explored in terms of a) coil-gap arrangement; and b) synchronization between driving currents of each coils. For coil-gap arrangement, calculation on the magnetic field distribution has been performed with various fixture gap cases. The guideline for calculation was good-field ( $\pm 0.1\%$ ) requirement of  $\pm 10$  mm. As for the synchronization of driving currents between two coils, two similar PFN (pulse-forming-network) systems were utilized to drive both coils with adjustable delay as a tuning knob. The effect of total current rise-time influenced by the time-lagging between two driving currents was examined and optimized. A specified synchronization requirement can be deduced accordingly.

### OPTIMIZATION OF FIXTURE GAP

A schematic layout of the dual one-turn coils configuration and the fixture gap between two coils is shown in Figure 1. During the test, the upper and lower coils were driven by separate pulse current from individual PFN units, respectively. An illustration of the extraction kicker cross-section of TLS (Taiwan Light Source) is given in Figure 2. For each regions in the figure (from center to outer rim), the white, skin, yellow and grey stand for the vacuum region of 40\*30 mm aperture, the ceramic chamber, the dual one-turn coils and the magnet ferrite, respectively.

Since the dimension of the existing ceramic chamber was fixed and the coils were located between ceramic chamber and the ferrite, the fixture gap was treated as a tuning variable in calculation while taking  $\pm 10$  mm good field region as the guiding constrain. The calculation was done by using POISSON [5]. Also, since the kicker magnet was designed and manufactured in window-frame, both the structure and calculated field distribution were symmetry on both horizontal and vertical axes. Consequently, only one quadrant of the magnet cross-section and the calculated field-line are displayed for illustration purpose.

A typical one quadrant of calculated field-line distribution of this dual one-turn coils configuration is shown in Figure 3. As indicated in the figure, the field-line gives uniform distribution within the center region of ceramic chamber (in skin color) where the good-field region is specified.

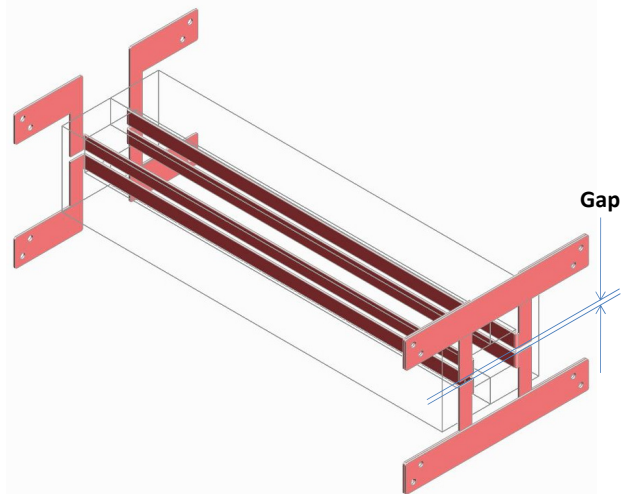


Figure 1: The dual one-turn coils configuration. The fixture gap is marked for illustration purpose.

The normalized magnetic field ratio of  $\Delta B/B_0$  in horizontal direction is shown in Figure 4, where  $B_0$  is the magnetic field strength at centre point and  $\Delta B$  is the difference between  $B_0$  and  $B(x)$  at  $x$ . Only vertical magnetic field is illustrated here for evaluation purpose. Various fixture gaps between the upper and lower coils were used in the calculation to estimate the corresponding  $\Delta B/B_0$  variation. These fixture gaps are engineering distinguishable and easy to fabricate. Nine fixture gaps were chosen for calculation, i.e. 0, 0.75, 1, 1.25, 1.5, 2, 3, 4 and 5 mm. The calculated results were analyzed and the corresponding relations of  $\Delta B/B_0$  curves are displayed in Figure 4. Each curve of  $g_0, g_{0.75}, g_1, g_{1.25}, g_{1.5}, g_2, g_3, g_4$  and  $g_5$  gives field variation with respect to the horizontal displacement ( $x$ ).

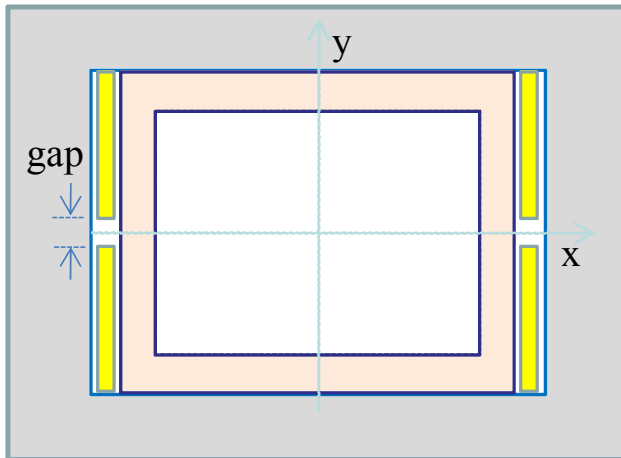


Figure 2: The cross section of TLS extraction kicker.

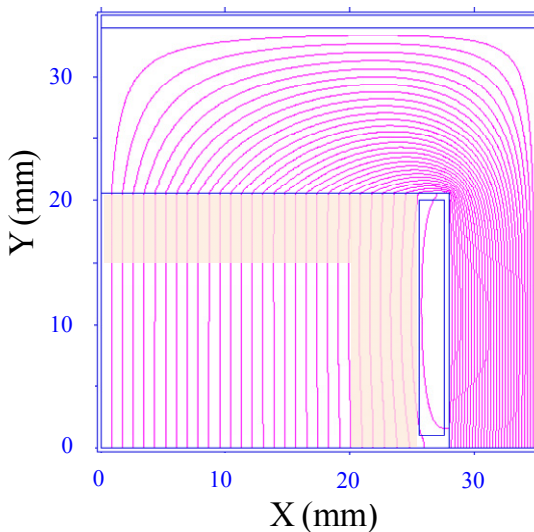


Figure 3: The typical one quadrant of magnetic field lines in the dual one-turn coils kicker magnet. The coil and ceramic chamber are also illustrated.

As shown in Figure 4, in the cases of  $gap \leq 1.25$  mm, the  $\Delta B/B_0$  becomes larger with increasing  $x$  as it moves away from the magnet center. Then, it decreases after

passing some high-value position. For those gaps  $\geq 1.5$  mm, the curves decrease with increasing  $x$ . The good field region is defined as  $\Delta B/B_0 \leq 0.1\%$  and is practically comparable with the commercial available power supplies stability. Using the calculated information provided in Figure 4, the relation between the available good field region and the fixture gap between two coils are further deduced and the result is given in Figure 5.

As shown in Figure 5, the good field region ( $x$ ) gets its largest value when the coil-gap is fixed at 1.2 mm. For all calculated coil-gaps, smaller or larger than 1.2 mm give less available good field region. Consequently, coil-gap = 1.2 mm is equipped in this case for further examination.

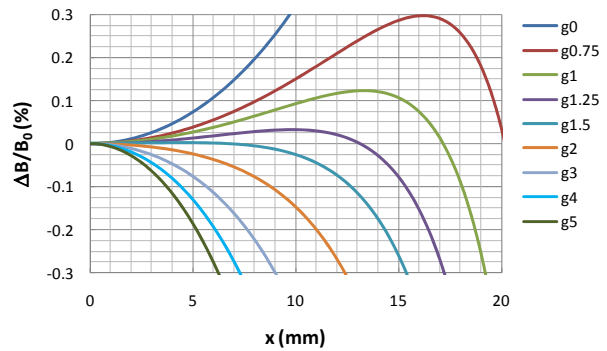


Figure 4: The normalized magnetic field ratio of  $\Delta B/B_0$  in horizontal direction.

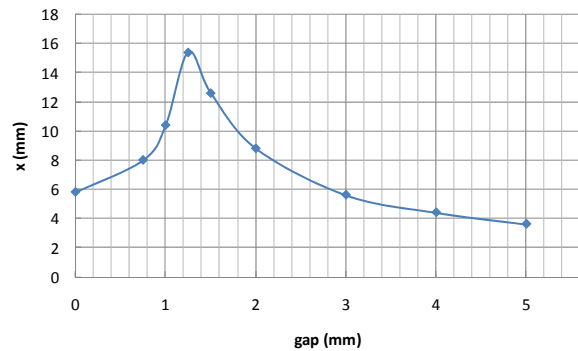


Figure 5: The relation between the good field region versus the gap between the two coils.

### TIME LAG

Two individual PFN units were used to energize the upper and lower coils respectively. The driving current of the kicker coils were monitored with current transformers (Pearson-101) and TDS-3054 scope (Tektronix). During the experiment, a DG-535 delay generator (Stanford) was used as the trigger source for both PFN units and for timing reference as well.

In order to explore the influence of synchronization effect between two driving current of upper and lower coils, an adjustable delay knob has been applied to provide the time-lag tuning capability. The total driving current of both coils provides the sum-up effect for this beam extraction kicker magnet.

A dual one-turn coils kicker magnet was fabricated and assembled for bench testing purpose, as shown in Figure 6. The fixture gap used in this assembling was 1.2 mm. A typical pulsed current delivering across either of the coils is given in Figure 7 and its associated rise-time was about 90 ns. Exploring the time-lag effect of the driving current between the coils was systematically examined by adjusting the delay knob in 20 ns step from 0 to 80 ns. The corresponding rise-time of the sum-up driving currents was recorded and the results are shown in Figure 8. The pairing of the time-lag and the corresponding rise-time of the driving currents were 0, 20, 40, 60, 80ns versus 90, 110, 135, 155 and 175ns, respectively. The rise-time of the sum-up driving current was linearly increased with the time-lag applied to the delay knob, as shown in Figure 9. It was interpreted as linear add-up of the two driving currents.

This dual one-turn coils configuration may be extended to multi-one-turn coils configuration, if needed, with examining practically for its fabrication feasibility.

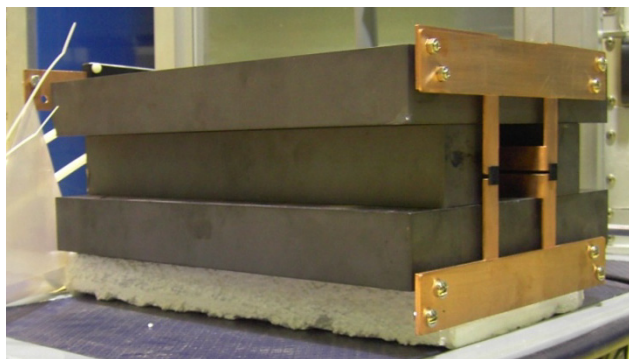


Figure 6: The dual one-turn coils kicker with ferrite.

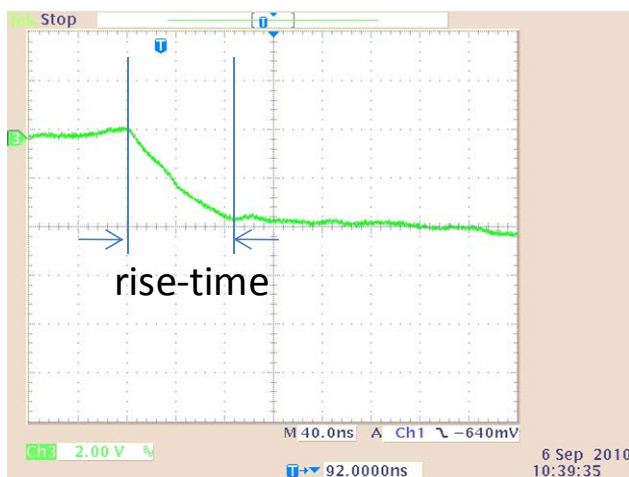


Figure 7: Typical rise-time of the driving current in dual one-turn coils kicker magnet.

### SUMMARY

The dual one-turn coils configuration for the extraction kicker magnet has been studied numerically in this study. The good field region of the kicker magnet was analyzed with respect to the fixture gap between the upper and

lower coils. Good field region was available for applying fixture gap between 1 and 1.8 mm. The sum-up current effect can be optimized by using a time-lag tuning knob and it is linearly add-up from the two individual driving current.

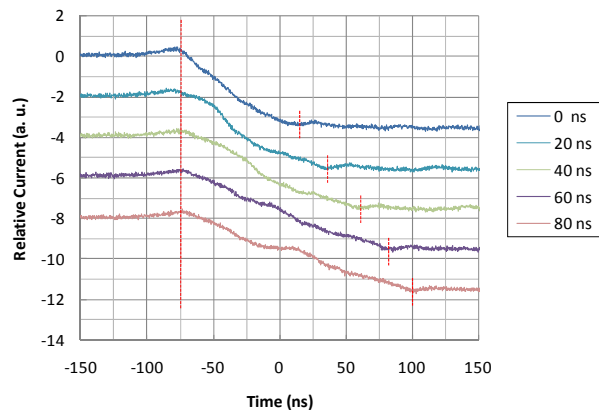


Figure 8: The sum-up current with time-lag of 0, 20, 40, 60 and 80 ns.

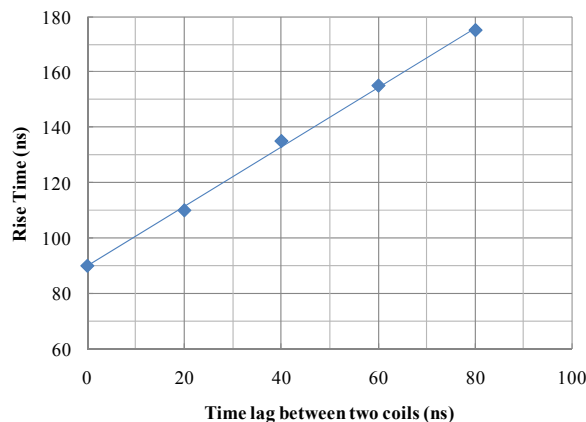


Figure 9: A linear relation between the rise-time and the time-lag.

### REFERENCES

- [1] E. Nakamura, “Fast-rise High-field Kicker Magnet Operating in Saturation”, Nucl. Instrum. Methods A 612, p. 50 (2009).
- [2] E. Nakamura, “Fast-rise High-field Multi-turn Coil Kicker Magnet Operating in Saturation”, Nucl. Instrum. Methods A 618, p. 22 (2010).
- [3] Toshiyuki Oki, “The bridged-T network lumped kicker: A novel fast magnetic kicker system for a compact synchrotron”, Nucl. Instrum. Methods A 607, p. 489 (2009).
- [4] K.L. Tsai, C. S. Fann, S. Y. Hsu, Y.S. Cheng, C.Y. Wu, K.H. Hu, Y.C. Liu, K.T. Hsu, K.K. Lin, C.T. Chen “Dual One-turn Coils for TLS Extraction Kicker Magnet”, IPAC-2010, p. 1796.
- [5] Los Alamos National Laboratory Poisson Superfish version 7 (2003)